CHAPTER 4

Chapter 4A

(a) Synthesis of MCM-48

(b) Loading of amino acids (L-Arginine & Cysteine) and drugs (Aspirin, Captopril and Camptothecin) into MCM-48

(c) Characterizations

J Porous Mater (2017) 24:1105–1115
DOI 10.1007/s10934-016-0351-4

Cysteine and *N*-acetyl cysteine encapsulated mesoporous silica: synthesis, characterization and influence of parameters on in-vitro controlled release

Soyeb Pathan[1] · Priyanka Solanki[1] · Anjali Patel[1]

Published online: 7 January 2017
© Springer Science+Business Media New York 2017

Abstract Pro-drug, cysteine loaded mesoporous silica materials with hexagonal (MCM-41) and cubic (MCM-48) geometry were synthesized by incipient wetness and soaking technique. The structure and properties of these synthesized materials were investigated by various physico-chemical techniques such as FT-IR, Nitrogen adsorption-desorption, XRD and TEM. An in-vitro release study of cysteine from these synthesized materials in SBF was carried out under stirring as well as static conditions. Effect of synthesis method as well as effect of geometry of carrier on release profile of drugs was also examined. Based on the obtained results for pro-drug, controlled release of real drug, N-acetyl cysteine was also carried out under optimized conditions. Release results shows that N-acetyl cysteine release was found to be more controlled as compare to that of cysteine from both mesoporous carriers. A study on release mechanism and release kinetics was also carried out using Higuchi model and first order release kinetic model.

Keywords MCM-41 · MCM-48 · Cysteine · *N*-acetyl cysteine · Controlled release · Kinetics

Electronic supplementary material The online version of this article (doi:10.1007/s10934-016-0351-4) contains supplementary material, which is available to authorized users.

✉ Anjali Patel
aupatel_chem@yahoo.com

[1] Department of Chemistry, Faculty of Science, The Maharaja Sayajirao University of Baroda, Vadodara, Gujarat 390002, India

1 Introduction

The construction of controlled-release systems for targeted drug delivery is of crucial importance for the development of both fundamental science and clinical medicine. In search of optimum drug delivery systems, variety of materials such as polymers [1], polymer based composites, bioactive glasses or ceramics [2, 3] has been frequently investigated. However, traditional disadvantage associated with mentioned systems i.e. disparate distribution of drug through these matrices, are clearly satisfied by mesoporous silica materials (M41S) as they possess ordered mesopores, high surface area, and well defined structure [4–7]. Studies also revealed that M41S have found potential applications for encapsulating bioactive molecules [8–11] and in domain of M41S family, extensive work has been carried out on MCM-41 as drug delivery carrier [12]. Among different bioactive molecules, release studies of ibuprofen from unfunctionalized and/or functionalized MCM-41 have been explored widely [13–19]. In spite of these, release of other molecules such as bisphosphonate [20], cytochrome C [21], cisplatin [22], Sulfadiazine [23], nifedipine [24], amino acids [25] from MCM-41 has also been reported.

The given reports suggested that factors such as the solubility of the drug in the solvent, the diffusivity of the drug in the solvent and the structure characteristics of the pore materials, pore diameter can seriously affect the release behaviors of the drug molecule. It was also shown that one-dimensional (1D) or three-dimensional (3D) cage-like pore structure with of mesoporous silica is of great benefit to control drug release [15]. In spite of these facts, less attention has been paid to other ordered mesoporous silica materials having different geometry e.g. cubic MCM-48 which contains three-dimensional channels. Qiu et al. have studied the release profile of

Journal of Porous Materials (2018) 25:1489–1498
https://doi.org/10.1007/s10934-018-0561-z

In vitro release of L-arginine and cysteine from MCM-48: a study on effect of size of active biomolecules on release rate

Priyanka Solanki[1] · **Anjali Patel**[1]

Published online: 19 January 2018
© Springer Science+Business Media, LLC, part of Springer Nature 2018

Abstract
The present paper consists of encapsulation of L-arginine as well as cysteine into MCM-48 with different amount and its characterization using various physicochemical techniques such as TEM, BET surface area, FT-IR, TGA, Powder XRD and ^{29}Si MAS NMR. The in-vitro release study of L-arginine as well as cysteine was carried out in simulated body fluid under static as well as stirring condition. A study on release kinetic as well as mechanism was also carried out using first ordered release kinetic model. The release profile of L-arginine and cysteine was co-related with the size and structure of biomolecules.

Keywords MCM-48 · L-arginine · Cysteine · In vitro-release · Effect of size and structure · Release kinetics and mechanism

1 Introduction

L-arginine and cysteine are essential amino acids. L-arginine involved in many biological process such as wound healing, tissue repaired, nitric oxide production etc., [1–12] and L-arginine intravenously administered to the patients with coronary artery disease to increase vascular NO bioavailability which show the vasodilatory effect. But the oral administrations of arginine do not show this effect. It is possible that the local availability of L-arginine as substrate for NO synthase may be reduce by the activity of arginase. Arginase utilizes L-arginine for the production of urea and ornithine and thus competes with NO synthase for substrate availability [3]. After administration of L-arginine, 40% is degraded in the intestine by arginase [4]. Cysteine is sulfur containing amino acid, acts as an antioxidant, and also involved in the production of glutathione. Reduction of this glutathione contributes to chronic inflammatory conditions, which are associated with cancer, neurogenerative, cardiovascular and infertility diseases resulting in high demand of cysteine [13, 14]. Cysteine pro-drugs are used to treat Schizophrenia and reduce drug cravings [15]. The administration of cysteine derivative such as *N*-acetylcysteine has major drawback of high dosage which can provoke persistent damage and strong allergic reactions [16–20].

As mentioned earlier, 40% L-arginine is degraded after oral administration and also required minimum three doses per day. For cysteine, also high dosages are required which may cause strong allergic reaction. The mention problems can be overcome if these biomolecules can be delivering in slow doses with controlled manner. This can only possible by using proper delivery carrier.

As M41S family have properties like higher surface area, ordered porosity, higher adsorption capacity, biocompatibility and non-cytotoxicity, they have been effectively explored as drug delivery carrier [21–24]. Among them a number of reports are available on MCM-41 and SBA-15 with functionalized or unfunctionalized form [25–50].

At the same time, very few reports are available on MCM-48, same member of the M41S family as drug delivery carrier [34, 50–53]. Recently, Cheng zhong Yu and his group have reported the release profile of Sulfasalazine from MCM-48 [54]. Zink et al. have reported the comparative study for release of hydrophilic dye (Rose bangal) and hydrophobic molecule [Camptothecin (CPT) and Rhodamine 6G (R6G)] from MCM-48 [55] Daniela Berger et al. have reported comparative study for release of aminoglycoside from MCM-48 [49].

As stated earlier, although L-arginine and cysteine are very important active biomolecules, only two reports are available: (1) adsorption of L-arginine on SBA-15 at different

✉ Anjali Patel
anjali.patel-chem@msubaroda.ac.in

[1] Department of Chemistry, Faculty of Science, The Maharaja Sayajirao University of Baroda, Vadodara, Gujarat 390002, India

Experimental

Materials

All chemicals used were of A. R. grade. 12-Tungstophosphoric acid (TPA), sodium hydroxide (NaOH), Cetyl trimethyl ammonium bromide (CTAB), Tetraethyl orthosilicate (TEOS), Ethanol, 32% Liquor Ammonia, NaCl, $NaHCO_3$, KCl, $K_2HPO_4.3H_2O$, $MgCl_2$. $6H_2O$, HCl, $CaCl_2$, Na_2SO_4 and $NH_2C(CH_2OH)_3$ were used as received from Merck. Ninhydrin, L-Arginine, Cysteine, Aspirin, Captopril and Camptothecin were used as received from Sigma Aldrich.

Synthesis of MCM-48

The synthesis of MCM-48 was carried out as reported in literature [1]. 2.4 g of CTAB was dissolved in 50 ml distilled water. To this, 50 ml ethanol (0.87 mole) and 12.6 ml ammonia (32 wt%, 0.2 mole) were added. The mixture was then stir for 10 min. When solution become homogenous, 3.4 g TEOS was added. After stirring for 2 h the resulting white solid was filtered and wash with distilled water. The template was removed by calcination for 823 K for 6 h. The resulting material was designated as MCM-48 (Figure 1).

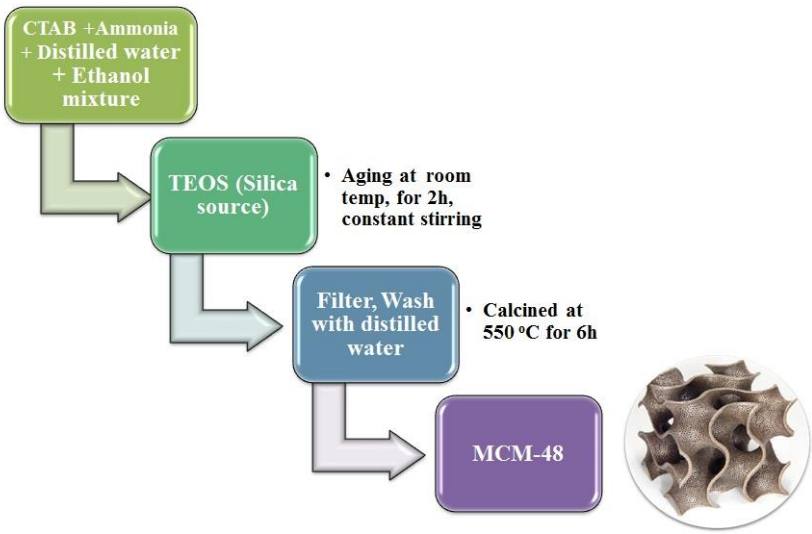

Figure 1. Synthesis of MCM-48

Loading of L-Arginine into MCM-48

Loading of L-Arginine was also carried out by same method, incipient wet impregnation as stated in experimental section of chapter 1A. The obtained material was designated as L-arg/MCM-48. Loading amount was further confirmed by thermal analysis which shows 0.1 g of L-Arginine was loaded per g of MCM-48.

Loading of Cysteine

Cysteine was loaded over MCM-48 using same method as stated in chapter 1A (by soaking and impregnation method). The obtained material was designated as Cys/MCM-48. The loading amount of Cysteine was obtained by analyzing the filtrate using UV–Vis spectroscopy as well as by thermal analysis which shows 14% loading of Cysteine into the MCM-41. Material prepared by incipient wetness impregnation method was designated as Cys/MCM-48(I).

Loading of drugs (Aspirin, Captopril and Camptothecin)

Loading of drugs were also carried out by same method as shown in chapter 1A. Aspirin, Captopril as well as Camptothecin were loaded into MCM-48 and designated as Cap/MCM-48, Asp/MCM-48 and CPT/MCM-48. The amount of drug loading was determined by analyzing filtrate at 296 nm, 203 nm and 370 nm respectively.

Results and Discussion

The synthesized MCM-48 and amino acids/drug loaded MCM-48 were characterized by various spectroscopic techniques such as TGA, FTIR, BET surface area, XRD and TEM.

Amount of loaded drug was obtained by two methods: (1) By UV-Visible spectroscopy analysis, which is by analyzing the obtained filtrate after loading at 296 nm, 203 nm and 370 nm for Aspirin, Captopril and Camptothecin respectively. Analysis of Cysteine loaded into MCM-48 were also carried out by same method by reacting it with ninhydrin reagent at 570 nm (2) By TG analysis of amino acids/drug loaded into MCM-48. The obtained results are shown in Table 1.

Table 1. Amount of amino acids/drug loaded into MCM-48

Amino Acid/Drugs	% Loading	Amount of amino acids/drug encapsulated (mg/g of carrier)
L-Arginine	10 ± 0.2	100 ± 2
Cysteine	14 ± 0.2	140 ± 2
Aspirin	4.8 ± 0.2	48 ± 2
Captopril	5.5 ± 0.2	55 ± 2
Camptothecin	8.0 ± 0.2	80 ± 2

TGA

Figure 2 shows TGA curves of MCM-48, L-arg/MCM-48, Cys/MCM-48, Asp/MCM-48, Cap/MCM-48 and CPT/MCM-48. TGA curve of MCM-48 shows initial weight loss of 0.7% up to 150 ^{o}C. This initial weight loss may be due to adsorption of physically adsorbed water molecules. After that no further weight loss is observed.

TGA curve of L-arg/MCM-48 shows initial weight loss of 0.85% which may be due to the presence of adsorbed water (Figure 2b). Further weight loss of 9.55% from 200 ^{o}C to 450 ^{o}C is observed which may be due to the removal of L-Arginine from MCM-48. TGA curve of Cys/MCM-48 (Figure 2c) shows initial weight loss of 2.2% due to the removal of adsorbed water. Further weight loss of 14% from 200 ^{o}C to 550 ^{o}C is observed which may be due to the removal of Cysteine from MCM-48.

TGA curve of Asp/MCM-48 initial weight loss of 2.5% up to 100 ^{o}C respectively which is corresponding to removal of adsorbed water. Further weight loss of 4.8% from 200 ^{o}C to 550 ^{o}C may be due to the removal of Aspirin from Asp/MCM-48.

TGA curve of Cap/MCM-48 initial weight loss of 2.7% up to 100 ^{o}C respectively which is corresponding to removal of adsorbed water. Further weight loss of 5.5% from 200 ^{o}C to 550 ^{o}C may be due to the removal of Cap from Cap/MCM-48.

TGA curve of CPT/MCM-48 initial weight loss of 4.5% up to 100 ^{o}C respectively which is corresponding to removal of adsorbed water. Further weight loss of 8.0% from 200 ^{o}C to 550 ^{o}C may be due to the removal of CPT from CPT/MCM-48.

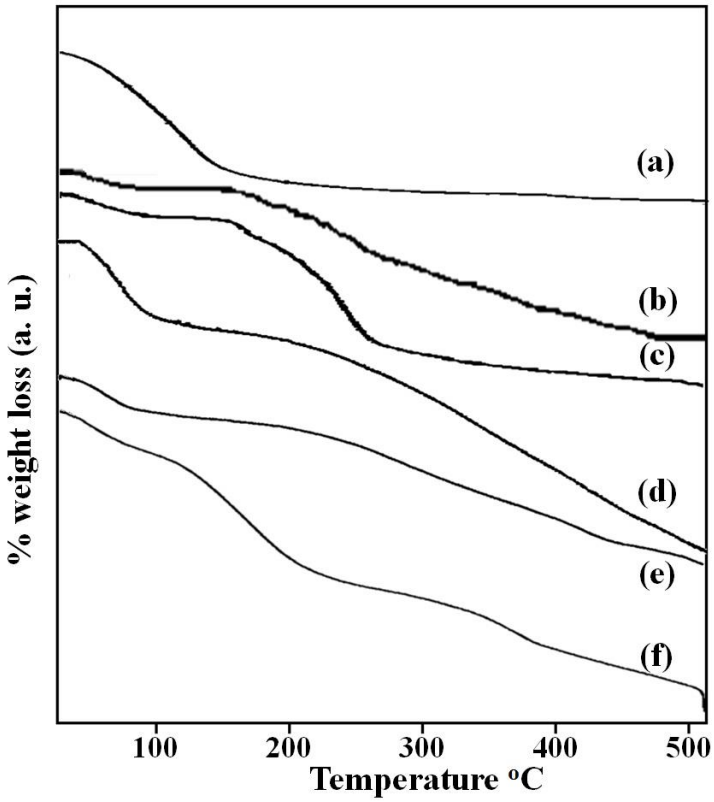

Figure 2. TGA curve of (a) MCM-48, (b) L-arg/MCM-48, (c) Cys/MCM-48, (d) Asp/MCM-48, (e) Cap/MCM-48 and (f) CPT/MCM-48

FTIR

The FTIR of MCM-48 (Figure 3) shows a broad band around 1100 and 1165 cm^{-1} corresponding to asymmetric stretching of Si-O-Si. The bands at 640 cm^{-1} and 458 cm^{-1} are due to symmetric vibrations of Si-O-Si and bending vibrations of Si-O, respectively.

The FTIR spectra of L-Arginine shows bands around 3103, 1680, 1558 cm^{-1} corresponds to N–H stretching vibration, NH_2 in plan bending vibration and C=O stretching vibration respectively [2]. All the peaks correspond to MCM-48 has been observed in FTIR spectra of L-arg_1/MCM-48. Further peaks correspond to L-Arginine has been observed with shifting in vibration band of NH_2 (from 1680 to 1666 cm^{-1}) and CO (from 1558 to 1442 cm^{-1}) group suggests the strong interaction of L-Arginine through this group with the surface Si-OH group of MCM-48.

The FTIR of Cysteine shows typical bands at, 2551 and 1589 cm^{-1} corresponds to SH, and CO respectively. Along with this, 1424 cm^{-1} and 1432 cm^{-1}, 1303 cm^{-1}, 1341

cm^{-1} corresponds to CH_2 in plan bending vibration, CH_2 stretching vibration, CH stretching vibration are observed [3]

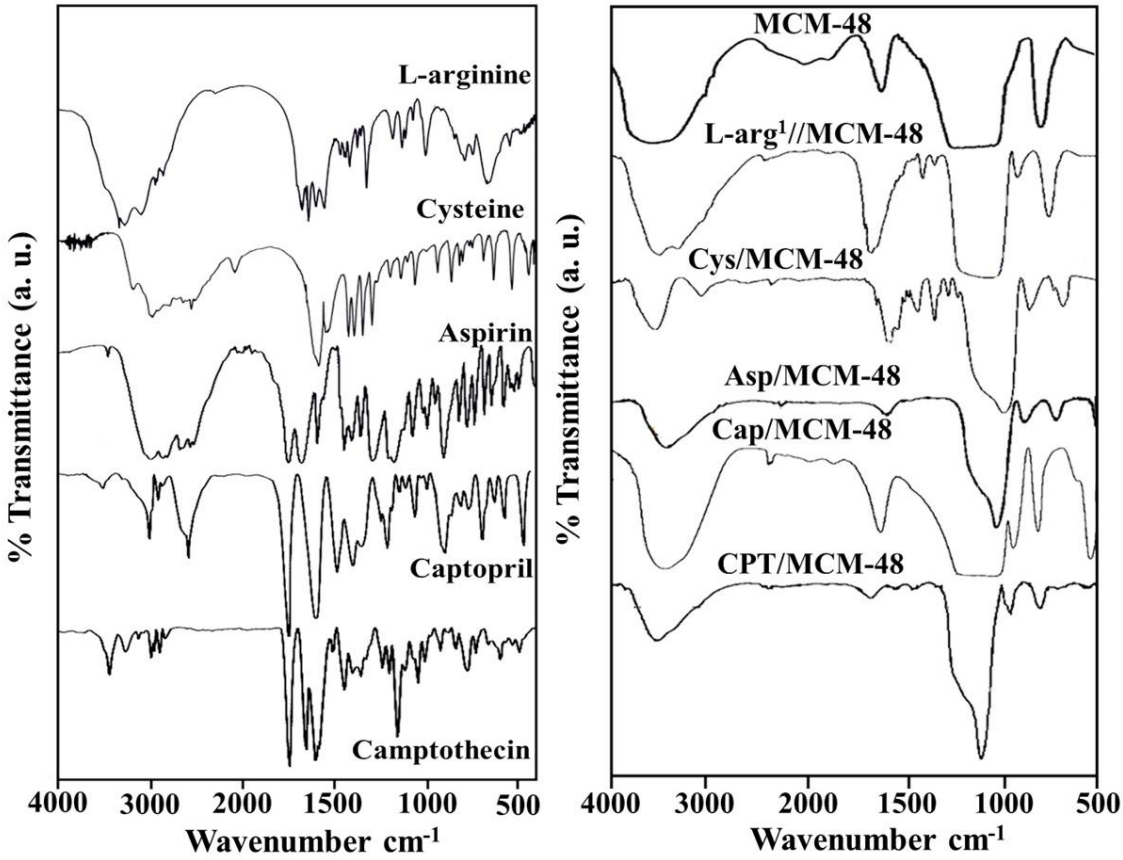

Figure 3. FTIR spectra of MCM-48, amino acids (L-Arginine and Cysteine), Drugs (Aspirin, Captopril and Camptothecin), and amino acids/drugs loaded MCM-48

The FTIR spectrum of Aspirin shows bands at 1630, 1020-1275, 545, 2700-2500 cm^{-1} and weak band at 2800-2600 cm^{-1} corresponding to C=O, C-O stretching and CO_2 rocking vibration and OH of carboxylic acid [4a, 4b]. The FTIR spectra of Asp/MCM-48 shows entire bands related to MCM-48. In additional to this it shows shifting in starching band of OH of carboxylic acid group to 2979 cm^{-1}. The bands corresponding to C=O and C-O stretching vibration may get merged with stretching vibration of Si-O-Si band. This also suggests homogeneous distribution of Aspirin molecules into the mesoporous channels of carrier.

The FTIR spectrum of Captopril shows bands at 2981, 2949 cm^{-1} for CH_3 and CH_2 asymmetric stretching, 2877 cm^{-1} for CH_3, 2567 cm^{-1} for SH, 1747 cm^{-1} for C=O of carboxylic acid, 1469 cm^{-1} for CH_3 bending vibration, 1228 cm^{-1} for C-N stretching vibration which are in good agreement with reported one [5]. FTIR spectrum of Cap/MCM-48 shows entire bands corresponding to MCM-48 suggesting the intact

structure of MCM-48 in Cap/MCM-48. Along with this, it shows shifting in band of SH and C=O groups from 2567 cm^{-1} to 2343 cm^{-1} and 1747 cm^{-1} to 1637 cm^{-1} respectively. This suggests the interaction of SH and C=O group of Captopril into MCM-41.

The reported bands of CPT are at 3425 cm^{-1}, 1736 cm^{-1}, 1648 cm^{-1}, and 1436 cm^{-1} corresponding to OH stretching, ester (carbonyl) stretch, carbonyl stretching and C-N stretching vibration, respectively [6]. FTIR spectrum of CPT/MCM-48 shows whole bands corresponding to MCM-48. Along with this, it shows bands shifting from 1736 to 1774 cm^{-1} corresponding to Ester (Carbonyl) which indicates the interaction of CPT with MCM-41 through ester carbonyl group.

Nitrogen adsorption-desorption isotherm

Nitrogen adsorption-desorption isotherm of all the materials are shown in Figure 4 and textural property of MCM-48 as well as all the loaded materials has been obtained using BET surface area analyzer and data are shown in Table 2. The isotherm is type (IV) in nature for all the systems which confirms the formation of mesoporous structure. Further it shows that structure of MCM-48 remain intact even after loading of amino acid/drugs.

Table 2. Textural properties of MCM-48 and amino acids/drug loaded MCM-48

Materials	**Specific surface area (m^2/g)**	**Pore volume (cm^3/g)**
MCM-48	1141	0.67
L-arg/MCM-48	109	0.25
Cys/MCM-48	541	0.41
Asp/MCM-48	705	0.26
Cap/MCM-48	344	0.29
CPT/MCM-48	187	0.32

The surface area of MCM-48 was found to be 1141 m^2/g with 0.7 cm^3/g pore volume. Decrease in surface are and pore volume is observed for all the amino acid/drug loaded systems, indicate the insertion of amino acid/drug into the mesoporous channels of MCM-48.

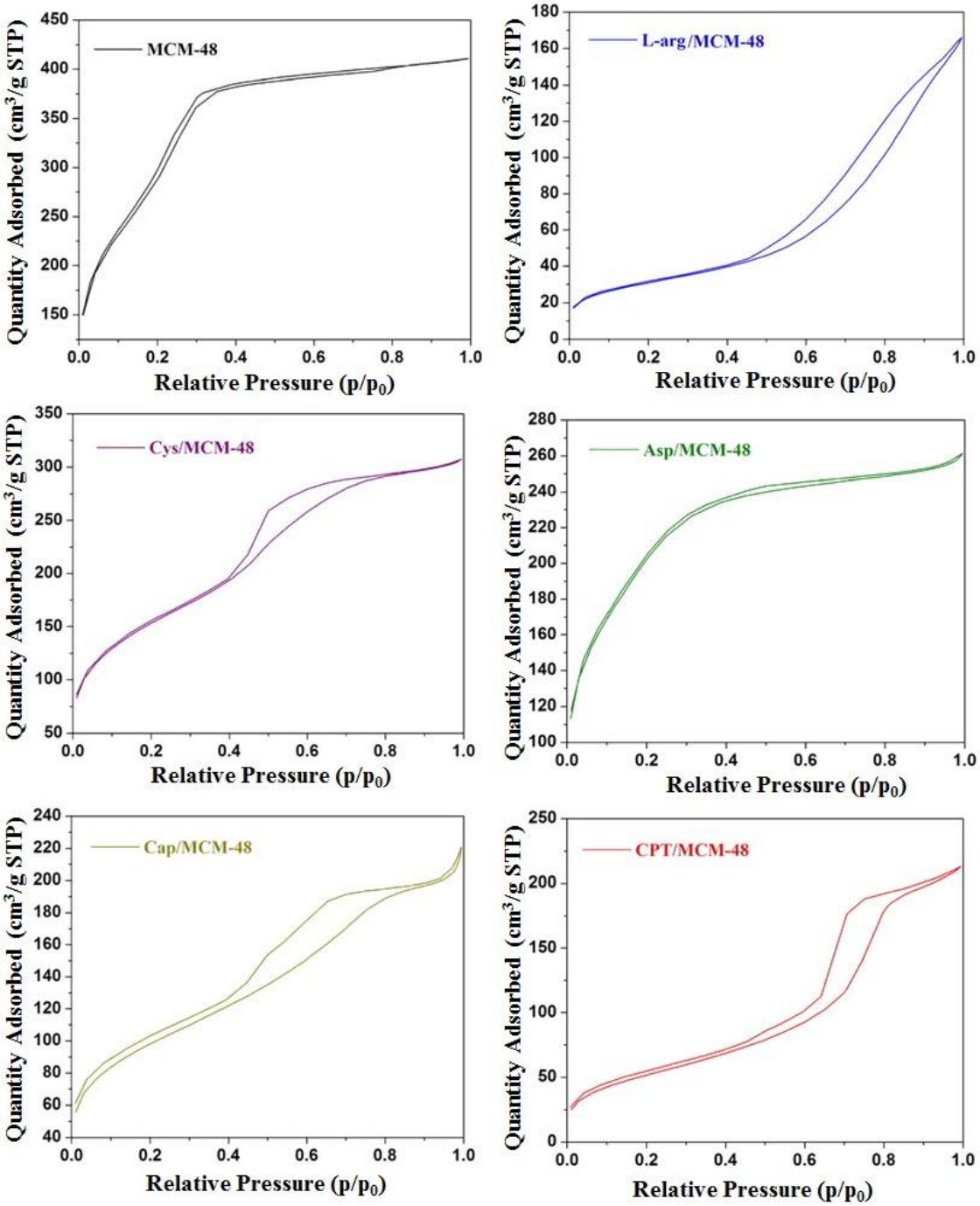

Figure 4. Nitrogen Adsorption-desorption isotherm of all materials

Low angle Powder XRD

Figure 5 shows powder XRD pattern of all materials. The XRD pattern of MCM-48 shows main characteristic peaks at 2.3^o which indicates the presence of intact structure of MCM-48. It also shows broad shoulder at 3.0^o corresponding to a plane 211 and 220, respectively. Several peaks in the range of 4-5^o diffraction angles correspond to the reflections of 400, 321 and 420 planes of a typical MCM-48 meso-structure with Ia3d cubic symmetry.

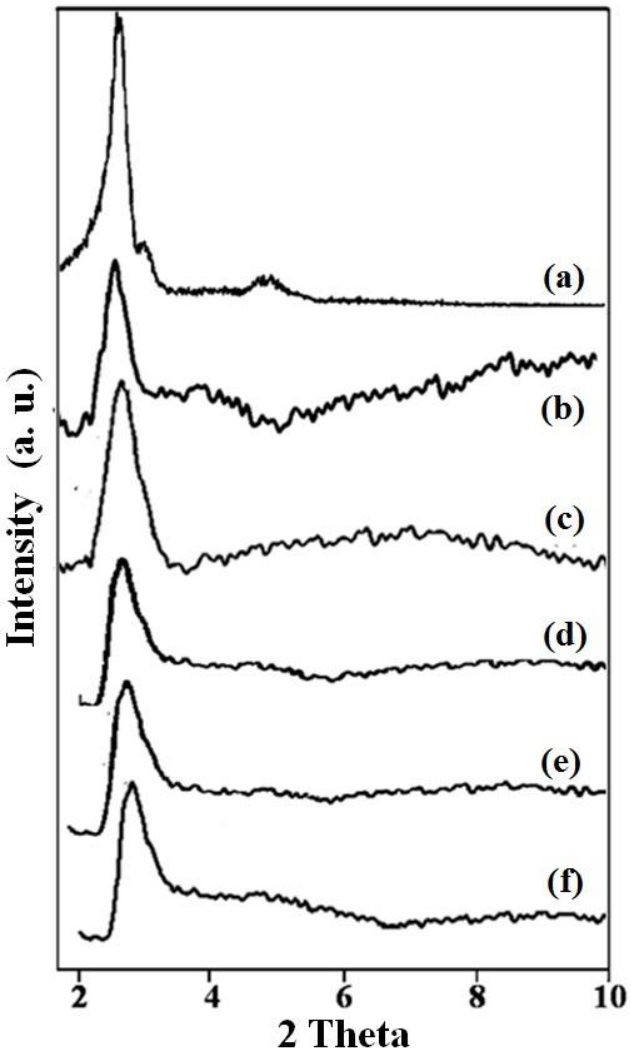

Figure 5. Low angle powder XRD of (a) MCM-48, (b) L-arg/MCM-48, (c) Cys/MCM-48, (d) Asp/MCM-48, (e) Cap/MCM-48 and (f) CPT/MCM-48

It is well known that the low angle XRD pattern are sensitive to pore filling and loaded materials show lowered intensity of characteristic peak compared to pure one. The main characteristic peaks at 2.3^o are also observed in amino acid/drug loaded samples with lower intensity. The intensity of rest of the peaks are very less in pure

MCM-48, which was further decrease in rest of the materials and disappears which suggests the insertion of L-Arginine and Cysteine into the mesoporous channels of MCM-48, good agreement with reported results [7, 8].

TEM

Figure 6 Shows TEM images of MCM-48, L-arg/MCM-48, Cys/MCM-48 Asp/MCM-48, Cap/MCM-48 and CPT/MCM-48 at 50 nm magnifications. TEM images of all the materials show spherical morphology. Further, loading of amino acid/drugs does not alter the structure of MCM-48. It also shows absence of any agglomeration indicating well-ordered homogenous dispersion of amino acids/drugs. However, L-arg/MCM-48 and Cys/MCM-48 shows porous structure with slight darkening as having higher loading.

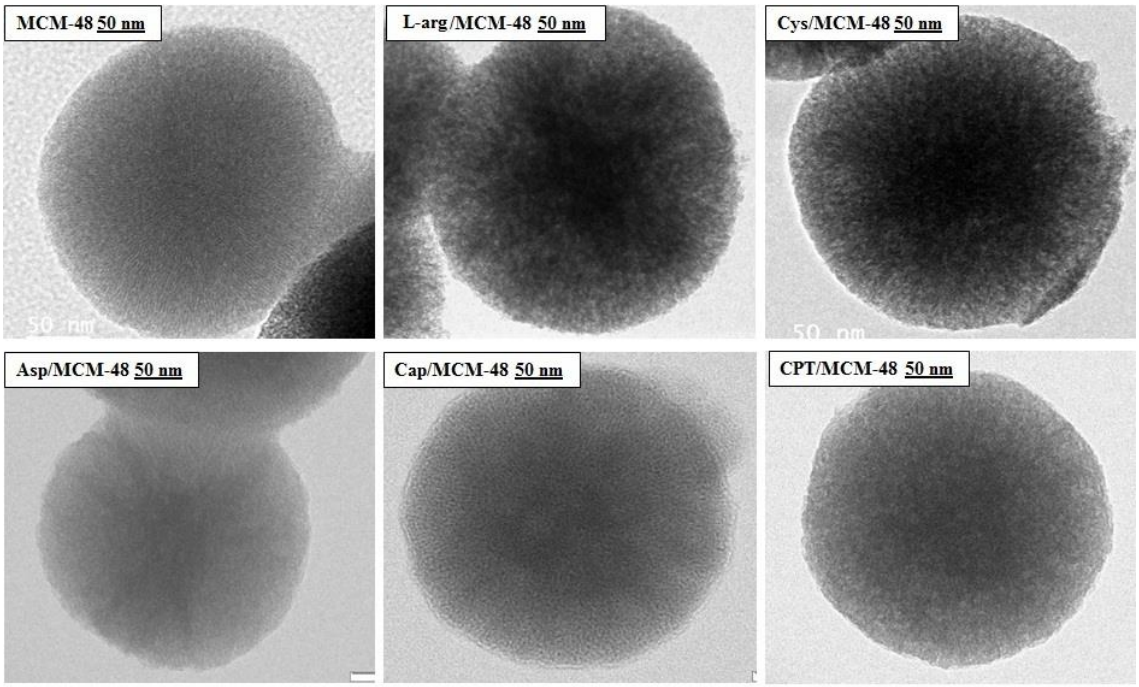

Figure 6. TEM images of MCM-48, L-arg/MCM-48, Cys/MCM-48, Asp/MCM-48, Cap/MCM-48 and CPT/MCM-48 at 50 nm magnification

Chapter 4B

(a) Functionalization of MCM-48 by 12-tungstophosphoric acid (TPA-MCM-48)

(b) Loading of amino acids (L-arginine & Cysteine) and drugs (Aspirin, Captopril and Camptothecin) into TPA-MCM-48

(c) Characterizations

Experimental

Functionalization of MCM-48 using 12-Tungstophosphoric acid (TPA)

MCM-48 was also functionalized by TPA using same method as describe in chapter 1B. 1 g of MCM-48 was impregnated with an aqueous solution of TPA (0.3/30 g/mL of distilled water) and dried at 100 ^{o}C for 10 h. The obtained material was designated as TPA-MCM-48.

Loading of Amino acids/drugs into TPA-MCM-48

Loading of L-arginine as well as Cysteine were carried out by same method as stated in chapter 1B. The prepared material was designated as L-arg/TPA-MCM-48 and Cys/TPA-MCM-48. Loading of drugs were also carried out by same method as mentioned in chapter 1B. The prepared material was denoted as Asp/TPA-MCM-48, Cap/TPA-MCM-48 and CPT/TPA-MCM-48. The loading amounts of amino acids/drugs were obtained by analyzing the filtrate using UV–Vis spectroscopy as well as by thermal analysis.

Results and discussion

Characterizations of TPA-MCM-48

The synthesized TPA-MCM-48 was characterized by various spectroscopic techniques. Only the main characterization techniques such as EDS, ^{29}Si and ^{31}P MAS NMR are presented here and the rest of the techniques will be discussed along with the drug loaded materials.

Elemental analysis (EDS)

EDS analysis for TPA-MCM-48 is shown in Table 1. The results obtained from EDS were in good agreement with the theoretical values.

Table 1 Results of elemental analysis in wt%.

Materials	Elemental analysis (weight %)			
	W		P	
	Theoretical	By EDS	Theoretical	By EDS
TPA-MCM-48	19.0	18.3	0.32	0.31

^{29}Si and ^{31}P MAS NMR

^{29}Si MAS NMR is a useful technique to study the chemical environment around the silicon nuclei in the mesoporous materials. Figure 1 represents the ^{29}Si MAS NMR spectra of MCM-48 and TPA-MCM-48. A broad peak of MCM-48 between -90 to -125 ppm observed which can be attributed to three main part of the peak with chemical shift at -92, -99 and -108 ppm (Figure 1a, Table 2). These signals resulted from Q^2 (-92 ppm), Q^3 (-99 ppm) and Q^4 (-108 ppm) silicon nuclei.

All the three, Q^2, Q^3 and Q^4 bands are observed in NMR spectra of TPA-MCM-48 (Figure 1b) suggesting the intact structure of MCM-48 even after functionalization. However, significant shift is observed in Q^2 band from -92 to -88 (Table 2) suggests the interaction of Si-OH group of MCM-48 with TPA.

Table 2 ^{29}Si chemical shift of MCM-48 and TPA-MCM-48

Sr. No.	Materials	^{29}Si MAS NMR data		
		Q^2 ppm	Q^3 ppm	Q^4 ppm
1.	**MCM-48**	-92	-99	-108
2.	**TPA-MCM-48**	-88	-98	-108

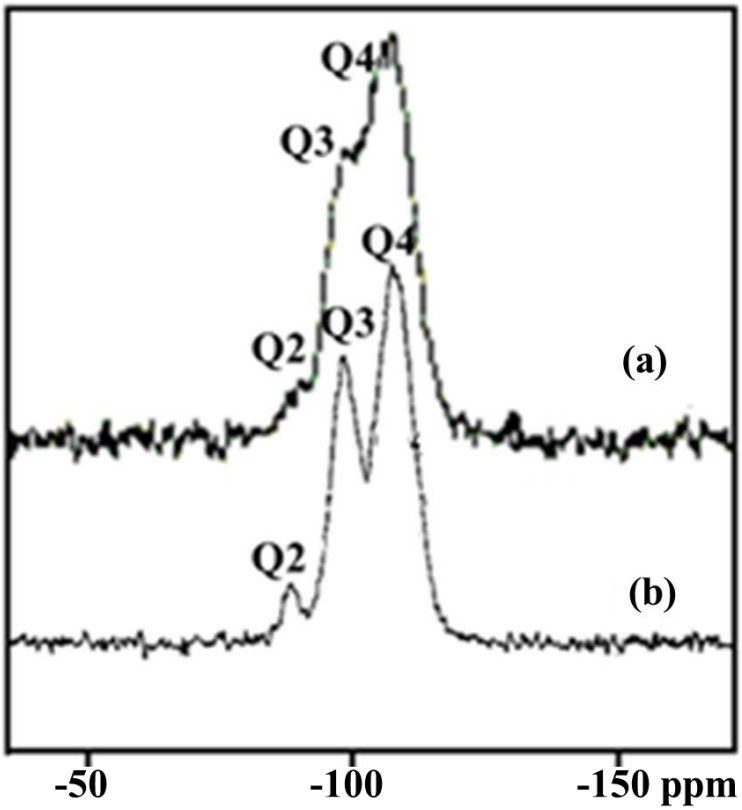

Figure 1 ^{29}Si MAS NMR of (a) MCM-48 and (b) TPA-MCM-48

^{31}P MAS NMR is the most important method to study chemical environment around the phosphorous in heteropoly compounds. The ^{31}P MAS NMR spectrum of TPA-MCM-48 is shown in Figure 2. The pure TPA shows single peak at -15.62 ppm [9]. The ^{31}P MAS NMR spectra of TPA-MCM-48 shows two peak at -12.27 and 3.060 ppm. The observed shift from -15.62 to -12.27 ppm is attributed to the strong interaction of MCM-48 with that of TPA as well as the presence of TPA inside the MCM-48. These results are in good agreement with reported one [10].

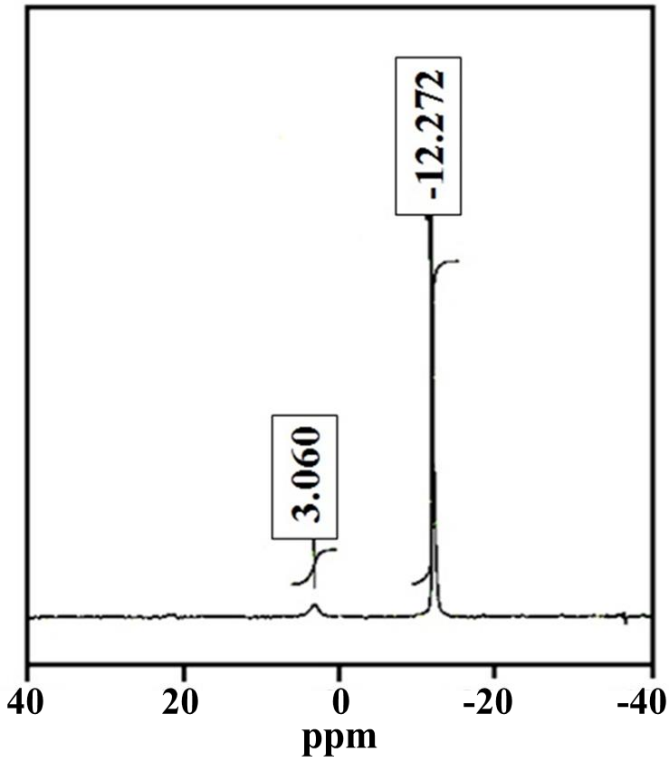

Figure 2. ^{31}P MAS NMR of TPA-MCM-48

Characterizations of drug loaded materials

All the drug loaded materials were characterized by various physicochemical techniques.

Amount of loaded drug was obtained by two methods: (1) By UV-Visible spectroscopy analysis, which is by analyzing the obtained filtrate after loading at 296 nm, 203 nm and 370 nm for Aspirin, Captopril and Camptothecin respectively. Analysis of cysteine loaded into MCM-48 were also carried out by same method by reacting it with ninhydrin reagent at 570 nm (2) By TGA analysis of amino acids/drug loaded into TPA-MCM-48. The obtained results are shown in Table 3.

Table 3. Amount of amino acids/drug loaded into TPA-MCM-48

Amino Acid/Drugs	% Loading	Amount of amino acids/drug encapsulated (mg/g of carrier)
L-arginine	10 ± 0.2	100 ± 2
Cysteine	8 ± 0.2	80 ± 2
Aspirin	3.6 ± 0.2	36 ± 2
Captopril	4.5 ± 0.2	45 ± 2
Camptothecin	7.5 ± 0.2	75 ± 2

TGA

Figure 3 shows TGA curves of (a) TPA-MCM-48, (b) L-arg/TPA-MCM-48, (c) Cys/TPA-MCM-48, (d) Asp/TPA-MCM-48, (e) Cap/TPA-MCM-48 and (f) CPT/TPA-MCM-48.

TGA curve of TPA-MCM-48 shows initial weight loss of 10-13% up to 150 ^{o}C which indicate presence of adsorbed water. Second weight loss of 1-2% between 200 and 300 ^{o}C corresponds to the loss of water of crystallization of Keggin ion. A gradual weight loss from 300 to 500 ^{o}C was observed due to the difficulty in removal of water present in TPA molecules inside the channels of MCM-48. This type of inclusion can cause the stabilization of TPA molecules inside the channels of MCM-48.

TGA curve of L-arg/TPA-MCM-48 shows initial weight loss of 2.45% up to 100 ^{o}C and further weight loss of 9.93% from 200 to 500 ^{o}C. Initial weight loss may be due to the presence of adsorbed water. Weight loss from 200 to 490 ^{o}C may be because of the removal of L-arginine from TPA-MCM-48.

TGA curve of Cys/TPA-MCM-48 also shows initial weight loss of 2.3% up to 150 ^{o}C respectively which is corresponding to removal of adsorbed water. Further weight loss of 8% from 200 ^{o}C to 550 ^{o}C may be due to the removal of cysteine from TPA-MCM-48.

TGA curve of Asp/TPA-MCM-48 shows initial weight loss of 2.7% up to 150 ^{o}C respectively which is corresponding to removal of adsorbed water. Further weight loss of 3.6% from 200 ^{o}C to 550 ^{o}C may be due to the removal of aspirin from TPA-MCM-48.

TGA curve of Cap/TPA-MCM-48 and CPT/TPA-MCM-48 also shows initial weight loss of 2.5% and 6.7% up to 150 ^{o}C respectively which indicates presence of adsorbed water. Further weight loss of 4.5% and 7.5% from 200 ^{o}C to 550 ^{o}C may be due to the removal of Captopril and CPT from TPA-MCM-48.

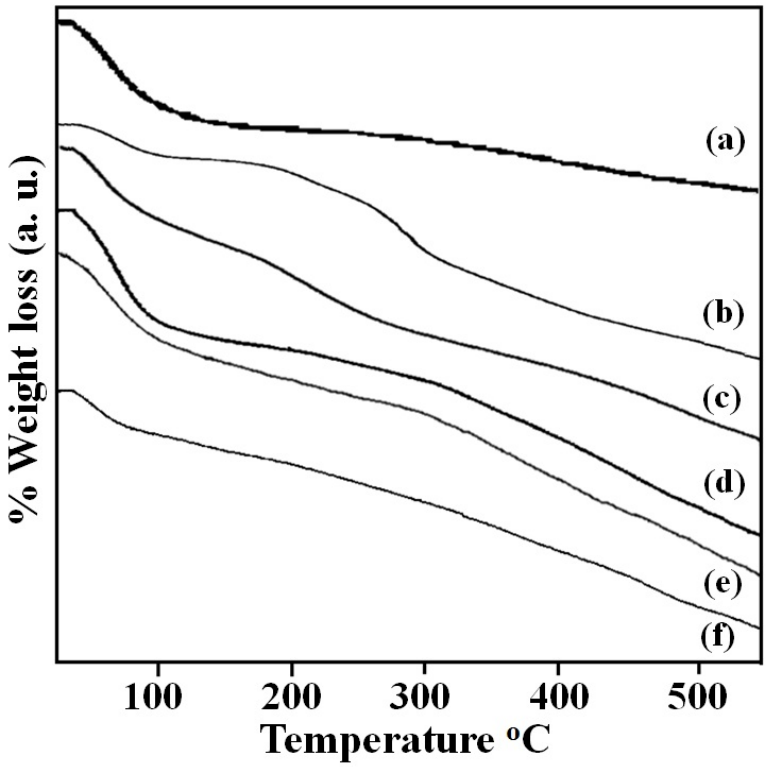

Figure 3. TGA curve of (a) TPA-MCM-48, (b) L-arg/TPA-MCM-48, (c) Cys/TPA-MCM-48, (d) Asp/TPA-MCM-48, (e) Cap/TPA-MCM-48 and (f) CPT/TPA-MCM-48

FTIR

FTIR bands of TPA-MCM-48, L-arg/TPA-MCM-48, Cys/TPA-MCM-48, Asp/TPA-MCM-48, Cap/TPA-MCM-48 and CPT/TPA-MCM-48 are shown in Figure 4. The reported bands for TPA are 1088, 987, and 897 cm^{-1} corresponding to P-O stretching, W=O symmetric stretching and W–O-W bending respectively. The presence of typical bands of TPA (R) at 982 cm^{-1} corresponding to Vas vibration of W = Od, and 897 cm^{-1} for stretching vibrations of W-O-W, in TPA-MCM-48 suggest the primary structure of TPA is remain intact even after functionalization of MCM-48. The absence of vibration band at 1080 cm^{-1} (V_s stretching of P-O) of TPA may be due to superimposition on the bands of MCM-48.

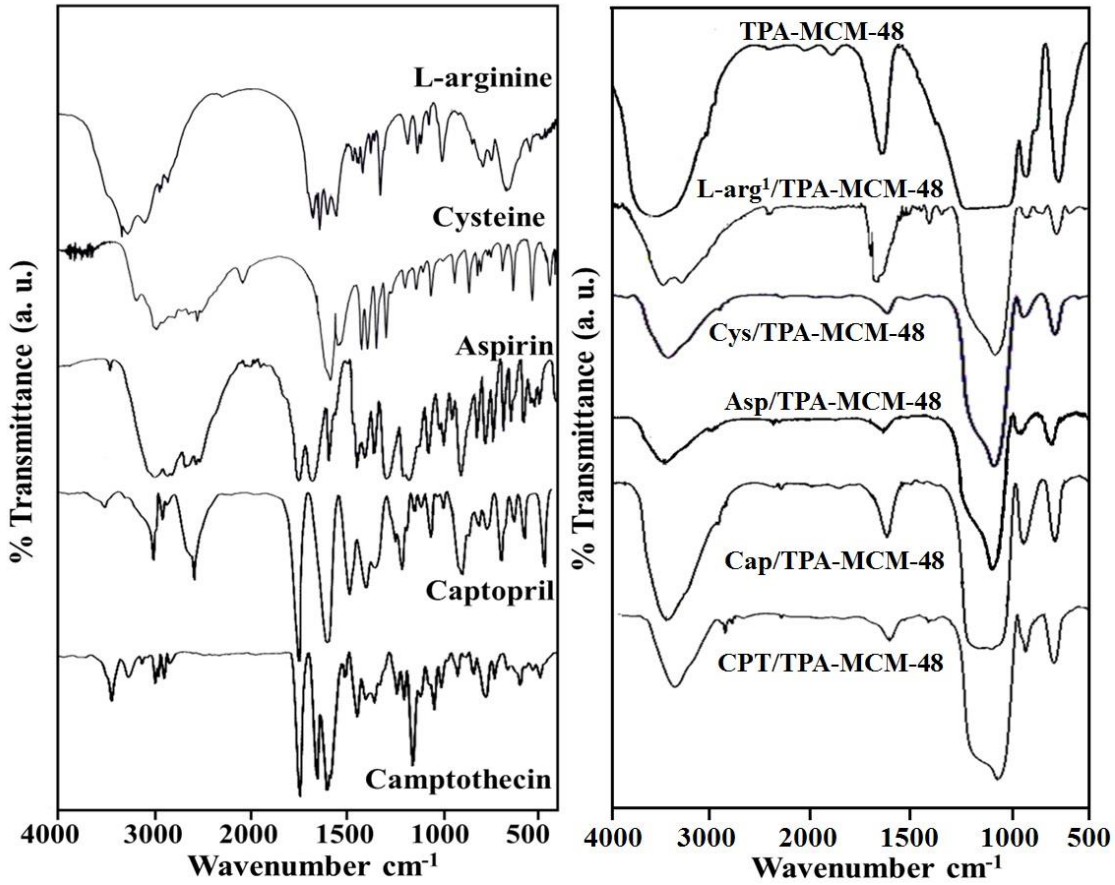

Figure 4. FTIR spectra of TPA-MCM-48, amino acids (L-arginine and Cysteine), Drugs (Aspirin, Captopril and Camptothecin), and amino acids/drugs loaded TPA-MCM-48

FTIR spectrum of L-arg/TPA-MCM-48 shows entire bands corresponding to TPA-MCM-48 with lower intensity suggests the structure of TPA-MCM-48 remains intact. It shows some additional bands at 3183 cm^{-1} due to the N-H stretching, 1690 cm^{-1} due to NH_2 in plane bending vibration and 1552 cm^{-1} due to C=O stretching vibration. Shifting in the bands correspond to C=O group and N-H group of L-arginine suggests the interaction of L-arginine to TPA-MCM-48 through these functional group.

FTIR spectrum of Cys/TPA-MCM-48 also shows whole bands related to TPA-MCM-48 suggesting the intact structure of TPA-MCM-48. The significant shifting in band of SH group from 2551 to 2600 cm^{-1} indicates the interaction of Cysteine through SH group.

The FTIR spectrum of Asp/TPA-MCM-48 shows entire bands related to TPA-MCM-48. In additional to this it shows shifting in starching band of OH of carboxylic acid group to 2980 cm^{-1}. The bands corresponding to C=O and C-O stretching

vibration may get merged with stretching vibration of Si-O-Si band. This also suggests homogeneous distribution of drug molecules into the mesoporous channels of carrier.

The FTIR spectrum of Cap/TPA-MCM-48 shows all bands corresponding to TPA-MCM-48 structure. Entire bands related to TPA-MCM-48 are present in Cap/TPA-MCM-48. Along with this shifting in band of SH and C=O groups are observed from 2567 cm^{-1} to 2310 cm^{-1} and 1747 cm^{-1} to 1631 cm^{-1} respectively. This suggests the interaction of SH and C=O group of captopril into MCM-41.

The FTIR spectrum of CPT/TPA-MCM-48 also shows whole bands related to TPA-MCM-48 which also indicates intact structure of TPA-MCM-48. It also shows shifting in band corresponding to ester carbonyl, from 1736 cm^{-1} to 1635 cm^{-1} which indicate the interaction of CPT with TPA-MCM-41 through C=O group.

Nitrogen adsorption-desorption isotherm

Figure 5 shows Nitrogen adsorption-desorption isotherm of TPA-MCM-48, L-arg/TPA-MCM-48, Cys/TPA-MCM-48, Asp/TPA-MCM-48, Cap/TPA-MCM-48 as well as CPT/TPA-MCM-48 and textural properties of these are shown in Table 4. The isotherm is type (IV) in nature according to the IUPAC classification which is a characteristic of mesoporous solids for all the six systems. This also suggests that functionalization as well as loading does not alter the structure of MCM-48.

Table 4. Textural properties of materials and amount of drug encapsulated into TPA-MCM-48

Materials	Specific surface area (m^2/g)	Pore volume (cm^3/g)
TPA-MCM-48	566	0.22
L-arg/TPA-MCM-48	68	0.10
Cys/TPA-MCM-48	222	0.210
Asp/TPA-MCM-48	299	0.19
Cap/TPA-MCM-48	296	0.20
CPT/TPA-MCM-48	108	0.06

Decrease in all structural parameters of amino acid/drug loaded TPA-MCM-48 suggests the insertion into the porous channels of TPA-MCM-48. Significant decrease in surface area and pore volume is observed in case of L-arg/TPA-MCM-48 as having maximum loading of L-arginine. In all the case, the basic structure of MCM-48 remains intact.

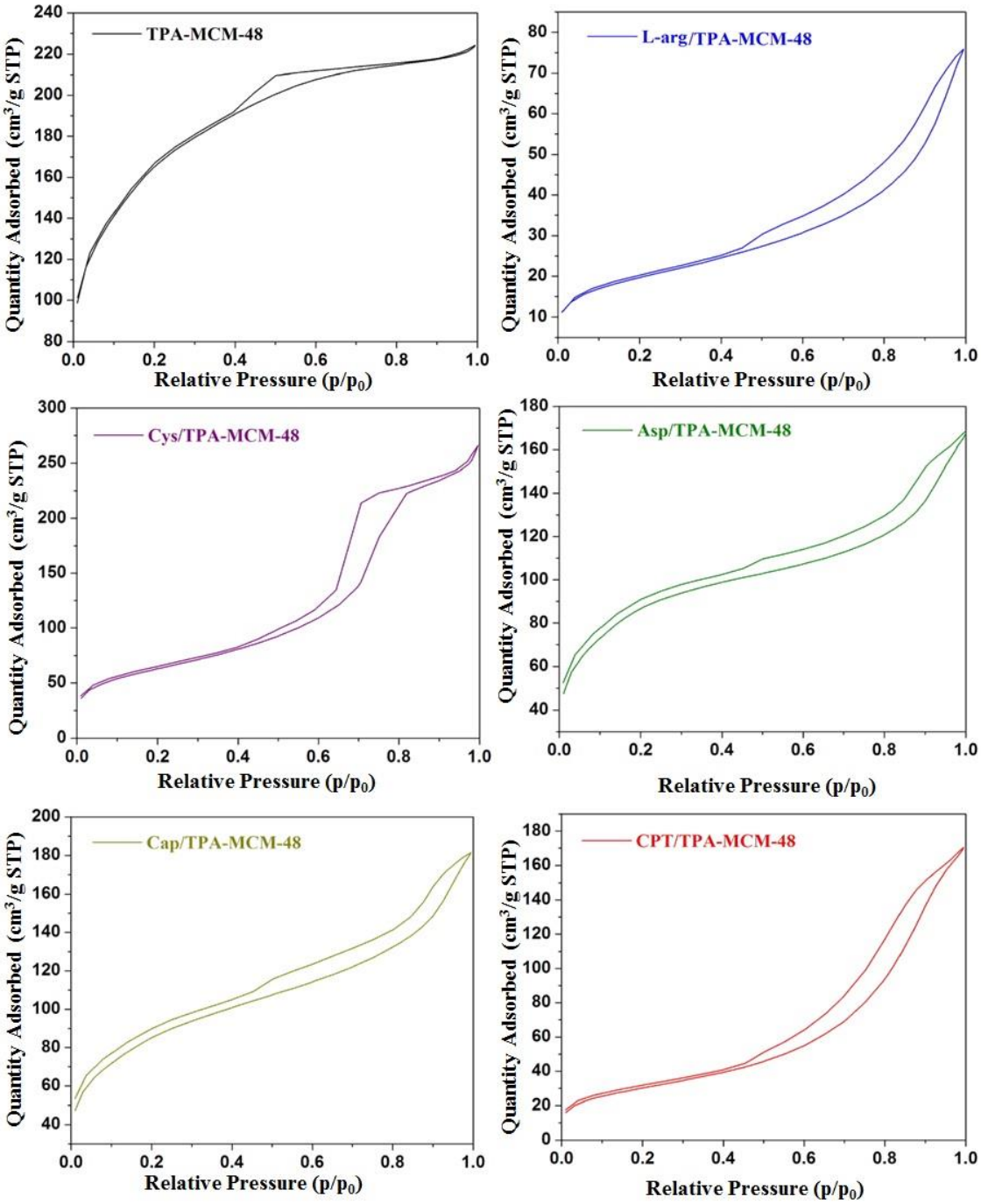

Figure 5. Nitrogen adsorption-desorption isotherms of all materials

Low Angle Powder XRD

Figure 6 shows low angle powder XRD of (a) TPA-MCM-48, (b) L-arg/TPA-MCM-48, (c) Cys/TPA-MCM-48, (d) Asp/TPA-MCM-48, (e) Cap/TPA-MCM-48 and CPT/TPA-MCM-48. It is well known that the low angle XRD pattern are sensitive to pore filling and loaded materials show lowered intensity of characteristic peak compared to pure one and this reflect in the XRD pattern of all the materials.

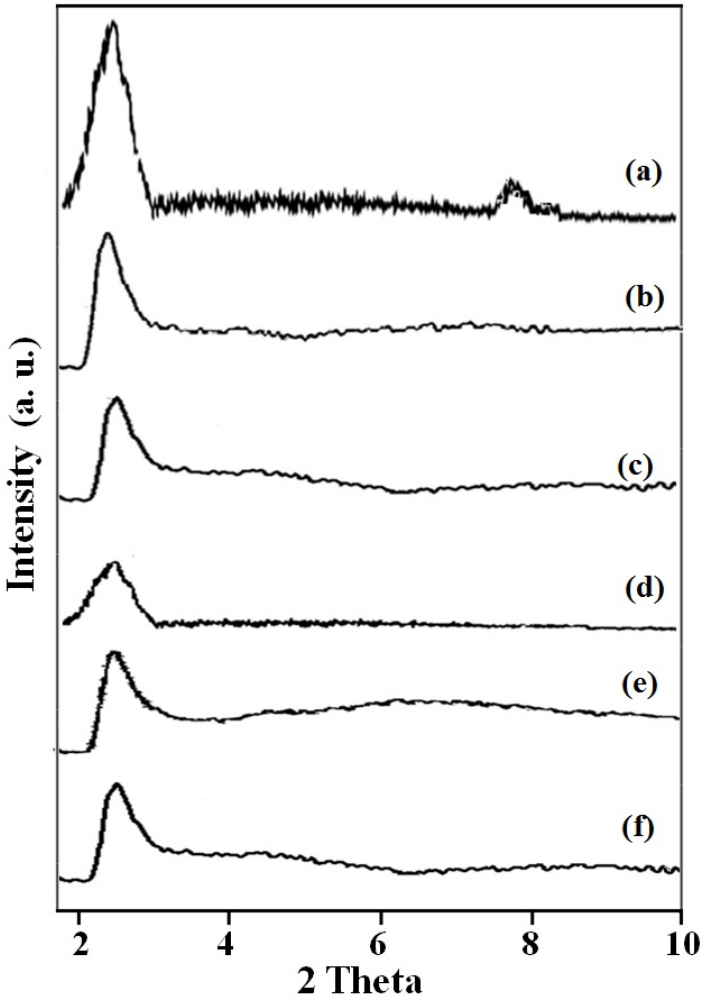

Figure 6. Low angle powder XRD of (a) TPA-MCM-48, (b) L-arg/TPA-MCM-48, (c) Cys/TPA-MCM-48, (d) Asp/TPA-MCM-48, (e) Cap/TPA-MCM-48 and (f) CPT/TPA-MCM-48

XRD pattern of all the materials shows characteristics peak at 2θ = 2.3° with lower intensity. Absence of any other peak indicates the insertion as well as homogeneous distribution of amino acids/drugs into the mesoporous channels of TPA-MCM-48. In addition to this, disappearance of secondary peak at 2θ = 3-5° in case of amino acid/drug loaded (Figure 6b-6f) was observed. This is because further loading of amino acids/drug into functionalized MCM-48 may block the channels which have already been confirmed by BET analysis. Further the hexagonal mesoporous structure of all the materials are confirmed by TEM (Figure 7).

TEM

Figure 7 shows TEM images of TPA-MCM-48, L-arg/TPA-MCM-48, Cys/TPA-MCM-48, Asp/TPA-MCM-48, Cap/TPA-MCM-48 and CPT/TPA-MCM-48 at 200 nm magnifications. The TEM image of TPA-MCM-48 shows similar spherical morphology

with porous system suggesting intact structure of MCM-48 even after functionalization. TEM images of rest of the materials also shows same morphology with spherical structure suggests that loading of amino acids/drugs does not alter the structure of TPA-MCM-48. Further, it also shows absence of any agglomeration which indicates well dispersion of drug into the mesoporous channels of the carrier.

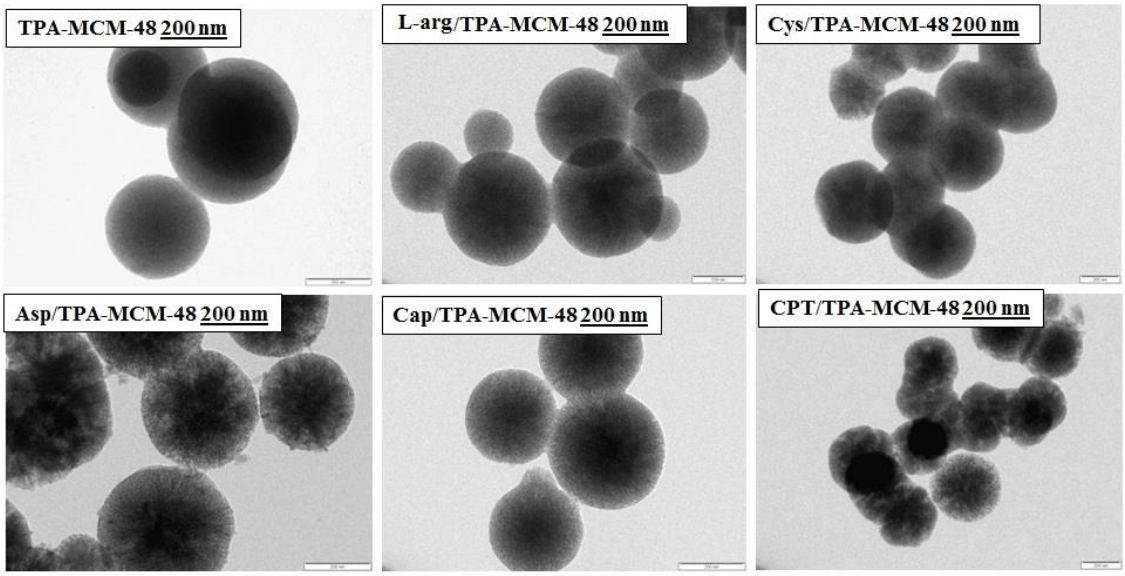

Figure 7 TEM images of TPA-MCM-48, L-arg/TPA-MCM-48, Cys/TPA-MCM-48, Asp/TPA-MCM-48, Cap/TPA-MCM-48 and CPT/TPA-MCM-48 at 200 nm magnification

Conclusion

- Synthesis of MCM-48 was successfully achieved by non-hydrothermal synthetic method and functionalization by wet impregnation method using TPA.
- Synthesis and functionalization was confirmed by elemental analysis and spectral studies.
- FTIR analysis shows that TPA interacts with MCM-48 through Si-OH group of MCM-48. Decrease in all parameters of BET surface area analysis shows the insertion of TPA into the mesoporous channels of MCM-48.
- Loading of amino acids/drugs have been successfully achieved by wet impregnation and soaking method.
- TGA and UV spectral studies gave the amount of amino acids/drugs loading into MCM-48 as well as TPA-MCM-48.
- FTIR analysis suggests the interaction between amino acids/drugs and carrier (MCM-48, TPA-MCM-48) which is mainly H-bonding.
- BET surface area analysis shows decrease in all parameters for amino acids/drugs loaded carrier which indicates insertion of amino acids/drugs into channels of carrier.
- Low angle powder XRD and TEM analysis show absence of agglomeration and homogeneous dispersion of amino acids/drugs into MCM-48 as well as TPA-MCM-48.

References

[1] D. Kumar, K. Schumacher, C.D.F.V. Hohenesche, M. Grun, K.K. Unger, Colloid Surf. A: Physicochem. Eng.Asp. 187-188, 109-116 (2001).

[2] S. Kumar, S.B. Rai, *Indian J. pure appl. Phys.* 48, 251 (2010).

[3] A. Patel, V. Brahmkhatri, In: M. Aliofkhazraei (Eds. 2015, vol 3),Comprehensive Guide for Mesoporous Materials, Properties and Development, Nova Science Publishers, Inc., pp. 271-284.

[4] (a) V. Renganayaki, S. Srinivasan, S. Suriya, Int J Chem Tech Res ISSN: 0974-4290, 4, 3 983-990 (2012). (b) I.G. Binev, B.A. Stamboliyska, Y.I. Binev, J. Mol. Struct. 378, 189 (1996).

[5] A.P. Imran, A.G. Nayan, R.R. Bhushan, S.P. Pawar, Int J pharm Sci 4:4, ISSN: 0976 (2013).

[6] A. Patil, S. Patil, S. Mahure, A. Kale, Am. J. Ethno. 1, 3, 174 (2014).

[7] A. Szegedi, M. Popova, I. Goshev, S. Kle´ bert , J. Miha´ly, J. Solid State Chem. 194, 257–263 (2012).

[8] B. Marler, U. Oberhagemann, S. Vortmann, H. Gies, Microporous Materials, 6, 375-383 (1996).

[9] T. Okuhara, N. Mizuno, M. Misono, Adv. Catal. 41, 113 (1996).

[10] S. Singh, A. Patel, Journal of Cleaner Production 72, 46 (2014).